Heavy-fermion behavior, crystalline electric field effects, and weak ferromagnetism in SmOs$_4$Sb$_{12}$

W. M. Yuhasz, N. A. Frederick, P.-C. Ho, N. P. Butch, B. J. Taylor, T. A. Sayles, and M. B. Maple

Department of Physics and Institute for Pure and Applied Physical Sciences, University of California San Diego,
La Jolla, California 92093, USA

J. B. Betts and A. H. Lacerda

National High Magnetic Field Laboratory/Los Alamos National Laboratory, Los Alamos, New Mexico 87545, USA

P. Rogl

Institut für Physikalische Chemie, Universität Wien, A-1090 Wien, Währingerstrasse 42, Austria

G. Giester

Institut für Mineralogie und Kristallographie, Universität Wien, A-1090 Wien, Althanstrasse 14, Austria

The filled skutterudite compound SmOs$_4$Sb$_{12}$ was prepared in single-crystal form and characterized using x-ray diffraction, specific-heat, electrical resistivity, and magnetization measurements. The SmOs$_4$Sb$_{12}$ crystals have the LaFe$_4$P$_{12}$-type structure with lattice parameter $a=9.3085$ Å. Specific-heat measurements indicate a large electronic specific-heat coefficient of ≈ 880 mJ/mol K^2, from which an enhanced effective mass m^* $\approx 170m_e$ is estimated. The specific-heat data also suggest crystalline electric field (CEF) splitting of the Sm^{3+} $J=5/2$ multiplet into a Γ_7 doublet ground state and a Γ_8 quartet excited state separated by ~ 37 K. Electrical resistivity $\rho(T)$ measurements reveal a decrease in $\rho(T)$ below ~ 50 K that is consistent with CEF splitting of ~ 33 K between a Γ_7 doublet ground state and Γ_8 quartet excited state. Specific-heat and magnetic susceptibility measurements display a possible weak ferromagnetic transition at ~ 2.6 K, which could be an intrinsic property of SmOs$_4$Sb$_{12}$ or possibly due to an unknown impurity phase.

I. INTRODUCTION

The family of filled skutterudite compounds exhibits a variety of interesting strongly correlated electron phenomena and have potential for thermoelectric applications. These phenomena include, for example, superconductivity in LaFe$_4$P$_{12}$,[1] heavy-fermion superconductivity in PrOs$_4$Sb$_{12}$,[2] ferromagnetism in SmFe$_4$P$_{12}$,[3] Kondo-insulating behavior in CeOs$_4$Sb$_{12}$,[4] and valence fluctuations in YbFe$_4$Sb$_{12}$.[5] The filled skutterudites have the chemical formula MT_4X_{12} where M=alkali metal, alkaline-earth, lanthanide, or actinide (Th or U); T=Fe, Ru, or Os; X=P, As, or Sb. The unit cell for these compounds consists of 34 atoms crystallized in a LaFe$_4$P$_{12}$-type structure with the $Im\bar{3}$ space group.[6]

The only Sm-based filled skutterudites to be characterized at low temperatures are all three phosphides and SmFe$_4$Sb$_{12}$; of these, only SmFe$_4$P$_{12}$ has been studied in single-crystal form.[3,7–14] These studies have revealed that SmFe$_4$P$_{12}$ is ferromagnetic below 1.6 K, SmRu$_4$P$_{12}$ has a metal-insulator transition at 16 K, SmOs$_4$P$_{12}$ is an antiferromagnet below 4.6 K, and SmFe$_4$Sb$_{12}$ is ferromagnetic below 45 K. Experiments on SmFe$_4$P$_{12}$ have also uncovered heavy-fermion and Kondo-lattice behavior, with a Kondo temperature of about 30 K and an electronic specific-heat coefficient of ~ 370 mJ/mol K^2.[3,9] By 7 T, the magnetization of SmFe$_4$P$_{12}$ at 1.8 K does not saturate and only reaches a value of 0.15 μ_B/f.u., which is much less than the Sm^{3+} free ion value of $M_{\text{sat}}=g_JJ$ μ_B=0.71 μ_B/f.u. This behavior was attributed to screening of the magnetic moment due to the

Kondo effect. Similar to SmFe$_4$P$_{12}$, the compound SmFe$_4$Sb$_{12}$ has also been found to be ferromagnetic; however, unlike the magnetization of SmFe$_4$P$_{12}$, SmFe$_4$Sb$_{12}$ is characterized by a saturation magnetization at 5 K of M_{sat} =0.7 μ_B/f.u., which agrees with the Sm^{3+} free ion value. After taking into account the contribution from the FeSb$_3$ polyanions, the effective magnetic moment of SmFe$_4$Sb$_{12}$ was found using Van Vleck's formula to be μ_{eff} =1.6±0.2 μ_B/f.u., in good agreement with the calculated value of μ_{eff}=1.66 μ_B/f.u.[14]

X-ray diffraction, specific-heat, magnetization, and electrical resistivity measurements on the compound SmOs$_4$Sb$_{12}$ have been performed.[15] These measurements revealed the presence of crystalline electric field effects, heavy-fermion behavior, and magnetic order. Analysis of the magnetization using scaling theory and modified Arrott plots shows signs of a ferromagnetic component to the magnetic order.

II. EXPERIMENTAL DETAILS

Single crystals of SmOs$_4$Sb$_{12}$ were grown in a molten Sb flux. Stoichiometric amounts of Sm (CERAC 99.9%) and Os (Colonial Metals 99.95%) were combined with an excess of Sb (CERAC 99.999%) in the atomic ratio 1:4:20 and placed in a carbon coated quartz tube, which was then evacuated and filled with 150 Torr Ar prior to being sealed. The sealed tube was placed in a box furnace, heated to 1050 ° C for 48 h, and then cooled to 700 ° C at 2 ° C/h. The resulting crystals were cubic and tended to form in large intercon-

TABLE I. Single-crystal structural data for $SmOs_4Sb_{12}$ ($LaFe_4P_{12}$-type, space group $Im\bar{3}$; No. 204) taken at $T=296$ K, with a scattering angle range of $2° < 2\theta < 80°$.

		$SmOs_4Sb_{12}$			
Crystal size	$84 \times 84 \times 56$ μm^3	Lattice parameter a [Å]	9.3085(2)	Density ρ [g/cm^3]	9.767
Reflection in refinements	$447 \leqslant 4\sigma(F_0)$ of 482	Number of variables	11	$R_F^2 = \Sigma|F_0^2 - F_c^2|/\Sigma F_0^2$	0.0207
Goodness of fit	1.284				
Sm in 2a (0, 0, 0);		Thermal displacements	[Å^2]	Interatomic distances [Å]	
Occupancy	1.00(2)	Sm: $U_{11} = U_{22} = U_{33}$	0.0552(6)	Sm–12 Sb	3.4824
Os in 8c (1/4, 1/4, 1/4);		Thermal displacements	[Å^2]	Interatomic distances [Å]	
Occupancy	1.00(1)	Os: $U_{11} = U_{22} = U_{33}$	0.0019(1)	Os–6 Sb	2.6241
Sb in 24g (0, y, z); y:	0.15589(3)	Thermal displacements	[Å^2]	Interatomic distances [Å]	
z:	0.34009(3)	Sb: U_{11}	0.0019(1)	Sb–1 Sb	2.9022
Occupancy	1.00(1)	U_{22}	0.0037(1)	1 Sb	2.9771
		U_{33}	0.0063(1)	2 Os	2.6241
				1 Sm	3.4824

nected clusters, with most of them much less than 1 mm in dimension. A small batch of ultra-high purity single crystals were also produced using Sm (AMES 99.99%), Os (Alfa Aesar 99.999%), and Sb (CERAC 99.999%). However, these single crystals were only used as a subsequent check for impurities.

The quality of the single crystals was determined by x-ray powder diffraction measurements, which were performed with a Rigaku D/MAX B x-ray machine on a powder prepared by grinding several-single crystals. Single crystal structural analysis was performed on two single crystals with similar dimensions. Inspection with an AXS-Gadds texture goniometer assured the high quality of the specimens prior to x-ray intensity data collection. For the data collection, a four-circle Nonius Kappa diffractometer equipped with a CCD area detector employing graphite monochromated Mo K_α radiation ($\lambda=0.071073$ nm) was used. Orientation matrix and unit cell parameters were derived using the DENZO program.[16] No absorption corrections were necessary because of the regular crystal shape and small dimensions of the investigated crystals. The structure was refined with the aid of the SHELXS-97 program.[17]

Specific heat $C(T)$ measurements were made between 0.6 and 70 K in a semiadiabatic ^{3}He calorimeter using a standard heat pulse technique. Many single crystals were combined for a total mass of 49.34 mg which were attached to the thermometer (Cernox)/heater sapphire platform with about 7.44 mg of Apiezon N grease. The electrical resistivity $\rho(T)$ of several samples with dimensions of $\sim 1 \times 0.5 \times 0.5$ mm was measured using a four probe technique from 1.1 to 300 K. Magnetoresistance $\rho(H,T)$ measurements were made using a four probe ac technique in fields up to 9 T in the 2 to 300 K temperature range in a Quantum Design Physical Properties Measurement System and in magnetic fields up to 18 T down to ~ 0.05 K using ^{3}He—^{4}He dilution refrigerators at UCSD (0–8 T) and the National High Magnetic Field Laboratory at Los Alamos National Laboratory (8–18 T). All of the resistivity measurements

were made with a constant current of 100–300 μA, perpendicular to the applied magnetic field. Magnetization measurements were made with Quantum Design superconducting quantum interference device magnetometers in the temperature range 1.7 to 300 K in magnetic fields up to 5 T. Measurements of the dc and ac magnetic susceptibility $\chi_{dc}(T)$ and $\chi_{ac}(T)$, respectively, and the isothermal magnetization $M(H)$ were made on a 5.37 mg single crystal with dimensions $\sim 0.6 \times 1.16 \times 1.18$ mm mounted such that the field was applied along the long axis of the crystal.

III. RESULTS

A. Single-crystal structural refinement

Analysis of the x-ray powder diffraction pattern indicated single phase $SmOs_4Sb_{12}$ with a minor impurity peak of $OsSb_2$ ($\lesssim 5\%$). Table I lists the results of a structural refinement performed on x-ray-diffraction data taken from two $SmOs_4Sb_{12}$ single crystals. The structural refinement indicated that $SmOs_4Sb_{12}$ has a $LaFe_4P_{12}$-type structure,[6] with a lattice parameter $a=9.3085$ Å and a unit cell volume of 806.6 Å^3. The Sm site was found to be fully occupied and Sm was found to have large isotropic thermal displacement parameters U_{ii} relative to those of Os and Sb. The values of U_{ii} for Sm are consistent with the "rattling" behavior of the filled skutterudite compounds.[18]

B. Specific heat

Displayed in Fig. 1(a) is a plot of the specific heat divided by temperature C/T vs T of $SmOs_4Sb_{12}$ between 0.6 and 25 K. Two features are readily apparent in the data represented by the open circles in Fig. 1(a). The first feature, a hump which peaks at ~ 2 K, can be associated with the onset of ferromagnetic order when corroborated by $\chi_{ac}(T)$ and $M(H)$ measurements described later in this article. The ferromagnetic ordering temperature (Curie temperature) was approximated by taking the maximum negative slope of C/T,
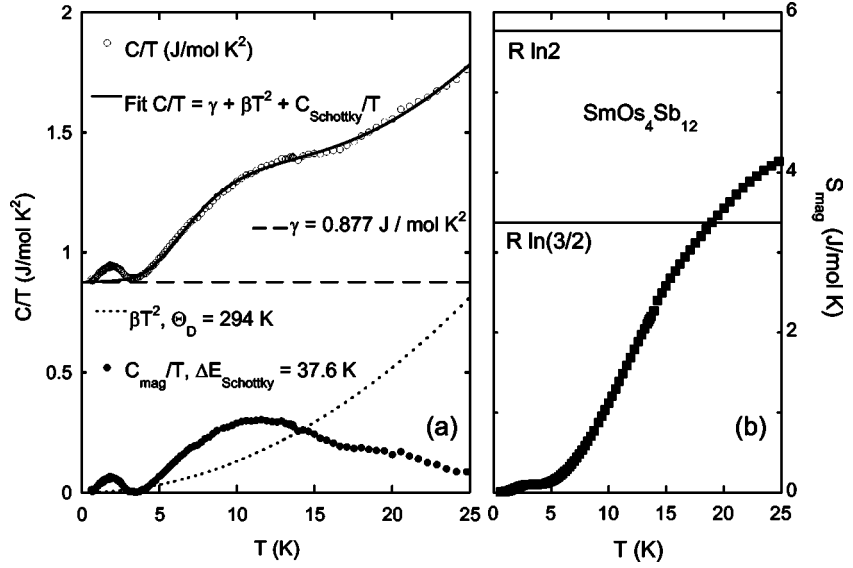
FIG. 1. (a) Plot of C/T vs T (open circles) and a fit to the data (solid line) that includes an electronic term (long dashed line), a lattice contribution (short dashed line), and a Schottky anomaly (see text for details). Also displayed is the magnetic contribution C_{mag}/T (filled circles), determined by subtracting the electronic and lattice terms from C/T. (b) Magnetic entropy S_{mag} of $SmOs_4Sb_{12}$ as a function of T.

which occurs at 2.6 K. This feature is not as well defined as that expected for a typical ferromagnetic transition and may be due to the presence of an impurity phase. However, this hump is similar to a broad feature in the specific heat of $PrFe_4Sb_{12}$ that is associated with the occurrence of magnetic order.[19]

The second feature observed in the specific-heat data is a Schottky-like anomaly centered at ~ 10 K. The data between 3.5 and 20 K were fitted by an equation containing electronic, lattice, and Schottky terms. These results are also displayed in Fig. 1(a). The Debye temperature $\Theta_D \approx 294$ K inferred from the fit is typical for a filled skutterudite compound, while the resultant electronic specific-heat coefficient $\gamma \approx 880$ mJ/mol K^2 is extremely large. It is important to note that this value of γ is fairly insensitive to the Debye temperature Θ_D and the splitting ΔE of the crystal field levels, changing by less than 5% for various reasonable values of Θ_D and ΔE. The effective mass m^* can be estimated from γ using the relation

$$\gamma = \frac{\pi^2 (Z/\Omega) k_B^2 m^*}{\hbar^2 k_F^2}, \tag{1}$$

where Z is the number of charge carriers per unit cell, Ω is the unit cell volume, and $k_F = (3\pi^2 Z/\Omega)^{1/3}$ is the Fermi wave vector using a spherical Fermi surface approximation. We assume that $Z=2$, since there are two formula units per unit cell and in each formula unit, Sm^{3+} contributes three electrons and each of the $(OsSb_3)^{-1}$ polyanions contributes one hole. Equation (1) yields $m^* \approx 170 m_e$, where m_e is the free electron mass, revealing that $SmOs_4Sb_{12}$ is a heavy-fermion compound.

The magnetic contribution to the entropy S_{mag} shown in Fig. 1(b) was determined by subtracting the electronic and lattice contributions from C/T, extrapolating to zero temperature, and then integrating over T. At the ~ 2.6 K magnetic transition, the magnetic entropy was found to be ~ 94 mJ/mol K (1.6% of $R \ln 2$) and it only reaches a value

of ~ 4.2 J/mol K by 25 K, where the Schottky contribution is in its high-temperature tail and significantly reduced.

C. Electrical resistivity

Electrical resistivity measurements were performed on several single crystals of $SmOs_4Sb_{12}$. Figure 2 displays the room-temperature normalized electrical resistivity $\rho/\rho(294$ K$)$ vs T for two representative samples. Samples A and B both exhibit metallic behavior with residual resistivity ratio (RRR) values of 12.7 and 19.1, respectively, and room-temperature resistivity $\rho(294$ K$)$ values of 313 and 379 $\mu\Omega$ cm, respectively. At low temperatures, there is a broad hump in $\rho(T)$ between 6 and 40 K for sample A and a kink in $\rho(T)$ at ~ 12.5 K for sample B. These features occur well above $T_{mag} \approx 2.6$ K determined from $C(T)$, as well as from $\chi_{ac}(T)$ and $M(H,T)$ data presented later. The sample dependence of the electrical resistivity along with the high room-temperature resistivity values indicate the presence of atomic disorder.

The temperature and magnetic field dependencies of the electrical resistivity for $SmOs_4Sb_{12}$ are shown in Figs. 3 and
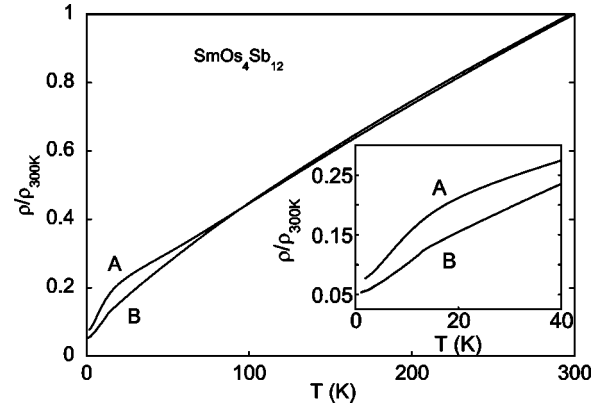

FIG. 2. Electrical resistivity ρ vs temperature T for $SmOs_4Sb_{12}$ samples A and B. The low-temperature behavior is shown in the inset.

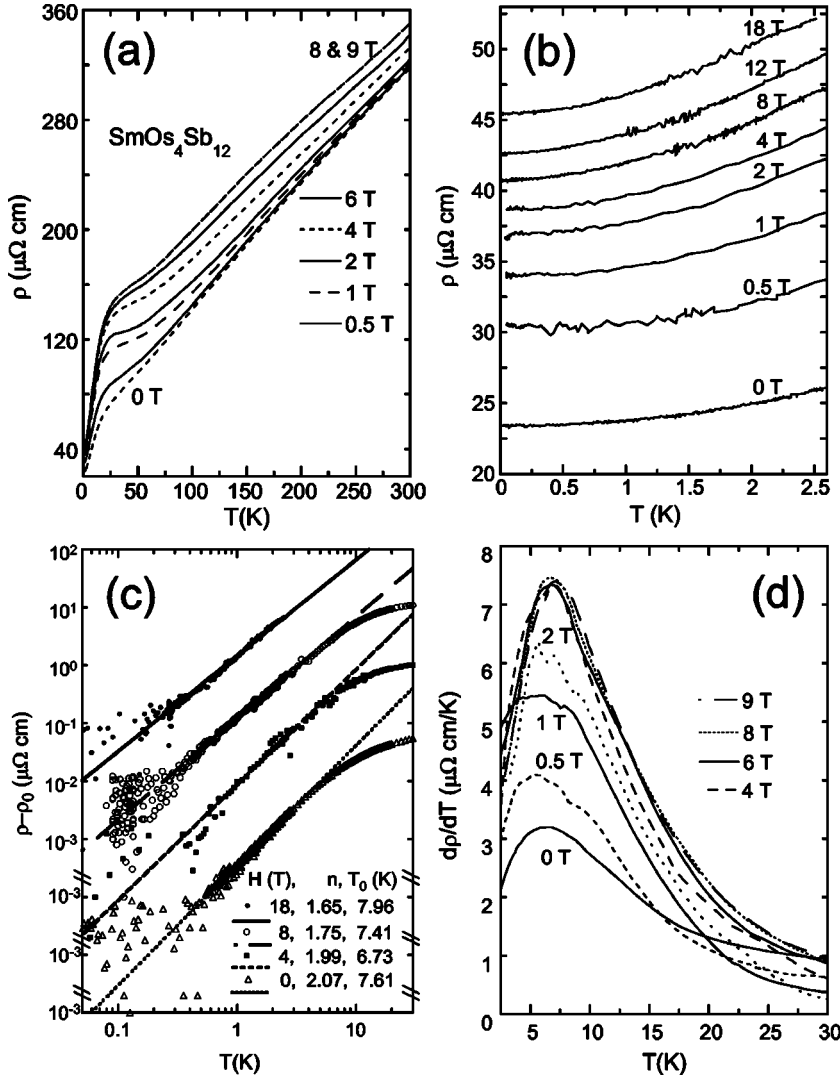FIG. 3. Electrical resistivity $\rho(T)$ at various fields for $SmOs_4Sb_{12}$ (Sample A). (a) $\rho(T,H)$ for $2\ K \leqslant T \leqslant 300$ K and $0\ T \leqslant H \leqslant 9$ T. (b) $\rho(T,H)$ for $0.02\ K \leqslant T \leqslant 2.5$ K and $0\ T \leqslant H \leqslant 18$ T. (c) $\rho - \rho_0$ vs T on a log-log scale. The lines are power law fits to the data of the form $\rho = \rho_0[1 + (T/T_0)^n]$. (d) $d\rho/dT$ vs T at fields up to 9 T showing a peak at ~ 7.5 K for all fields.

4. Figure 3(a) displays the electrical resistivity of $SmOs_4Sb_{12}$ from 2 to 300 K in fields up to 9 T. In general, the resistivity increases with increasing field at all temperatures. The shoulder in $\rho(T)$, which is observed at ~ 30 K, becomes more prominent as the magnetic field increases. The behavior of the low-temperature $\rho(H)$ data above 4 T for $SmOs_4Sb_{12}$ is very similar to that of $LaOs_4Sb_{12}$; however, below 4 T, the $\rho(H)$ data exhibit a rapid increase with H whose origin is not understood.

The heavy fermion behavior inferred from the specific-heat measurements is also reflected in the electrical resistivity. The electrical resistivity of a typical f-electron heavy-fermion compound has a relatively weak temperature dependence at high temperatures and then decreases rapidly with decreasing temperature below a characteristic "coherence temperature," until, at the lowest temperatures, the resistivity varies as T^2. The T^2 dependence is indicative of Fermi-liquid behavior and is strong enough to be readily observable in most heavy-fermion compounds. In order to ascertain whether the resistivity of $SmOs_4Sb_{12}$ follows this T^2 dependence at low temperatures, power-law fits of the form $\rho = \rho_0[1 + (T/T_0)^n]$ (where ρ_0 is the residual resistivity and T_0 is a characteristic temperature) were made to the $\rho(T)$

data in the temperature range from ~ 0.05 to ~ 10 K up to 8 T and from ~ 0.02 to 2.6 K from 10 to 18 T [Fig. 3(c)]. The fits show that the exponent n is approximately 2 up to 4 T, consistent with Fermi-liquid behavior, and then decreases with increasing field, possibly indicating a cross over to field-induced non-Fermi-liquid behavior. The value of T_0 determined from the power-law fits varies between ~ 7 and 8 K, and may be associated with the peak observed in the derivative of the resistivity $d\rho/dT$ vs T, shown in Fig. 3(d), which occurs around 7.5 K at all fields between 0 and 9 T. This low value of the scaling temperature T_0 is consistent with the large value of γ.

The coefficient $A\ [=\rho_0/(T_0^2)]$ of the T^2 term in the electrical resistivity is often found to follow the Kadowaki-Woods (KW) relation $A/\gamma^2 = 1 \times 10^{-5}\ \mu\Omega$ cm mol^2 K^2 mJ^{-2} (where γ is the electronic specific heat coefficient).[20] For $SmOs_4Sb_{12}$, the power-law fits to the electrical resistivity result in an A/γ^2 ratio of $\sim 0.5 \times 10^{-6}\ \mu\Omega$ cm mol^2 K^2 mJ^{-2} at 0 T, which is ~ 20 times smaller than the value expected from the KW relation. However, Tsujii *et al.* recently found a different empirical relation $A/\gamma^2 \approx 0.4 \times 10^{-6}\ \mu\Omega$ cm mol^2 K^2 mJ^{-2}, from studies of several Yb-based compounds (such as $YbCu_5$, $YbAl_3$, and $YbInCu_4$), some Ce-based compounds ($CeNi_9Si_4$ and $CeSn_3$), and some
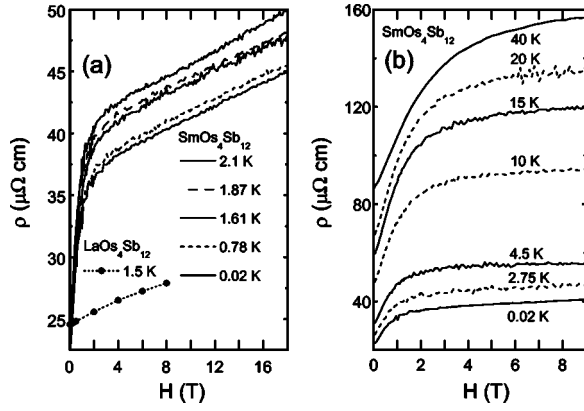
FIG. 4. Electrical resistivity $\rho(H)$ at various temperatures for SmOs$_4$Sb$_{12}$ (sample A) along with $\rho(H)$ at 1.5 K for LaOs$_4$Sb$_{12}$. (a) $\rho(H,T)$ for 0 T$\leqslant H\leqslant$9 T and 0.02 K$\leqslant T\leqslant$40 K. (b) $\rho(H,T)$ for 0 T$\leqslant H\leqslant$18 T and 0.02 K$\leqslant T\leqslant$2.75 K. The $\rho(H)$ data for LaOs$_4$Sb$_{12}$ (solid circles) at 1.5 K (shifted upwards by adding 20 $\mu\Omega$ cm) for comparison with the low-temperature $\rho(H)$ data of SmOs$_4$Sb$_{12}$.

transition metals (such as Fe, Pd, and Os).[21] To explain this new relation, Tsujii *et al.* suggested a relation to the ground-state degeneracy of the system, which has been developed further by Kontani in the form of a generalized Kadowaki-Woods relation.[21,22] The A/γ^2 value for SmOs$_4$Sb$_{12}$ seems to be in much better agreement with this new relation and, thereby, consistent with the behavior of several other heavy-fermion compounds.

D. Magnetization and magnetic susceptibility

Inverse dc magnetic susceptibility χ_{dc}^{-1} vs T data for SmOs$_4$Sb$_{12}$ are shown in Fig. 5. Since Sm^{3+} ions have relatively low-energy angular momentum states above the Hund's rule $J=5/2$ ground state, a simple Curie-Weiss law
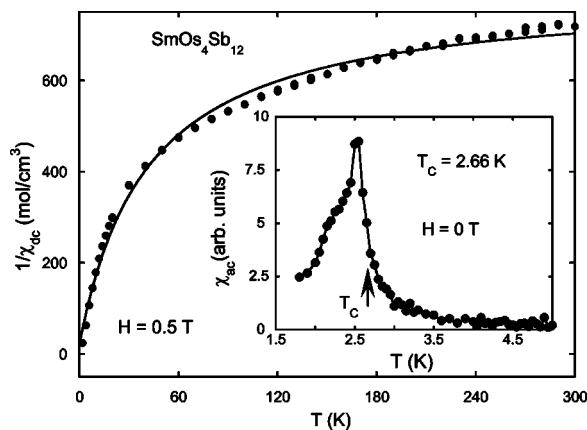

FIG. 5. Inverse dc magnetic susceptibility χ_{dc}^{-1}, measured at 0.5 T, vs temperature T (filled circles) for SmOs$_4$Sb$_{12}$. The line represents a fit of a Curie-Weiss law with a temperature-independent Van Vleck term using Eq. (2) to the $\chi_{dc}^{-1}(T)$ data. The inset shows the temperature dependence of the ac magnetic susceptibility χ_{ac}. The arrow denotes the T_C of SmOs$_4$Sb$_{12}$ (defined as the midpoint of the transition on the paramagnetic side).
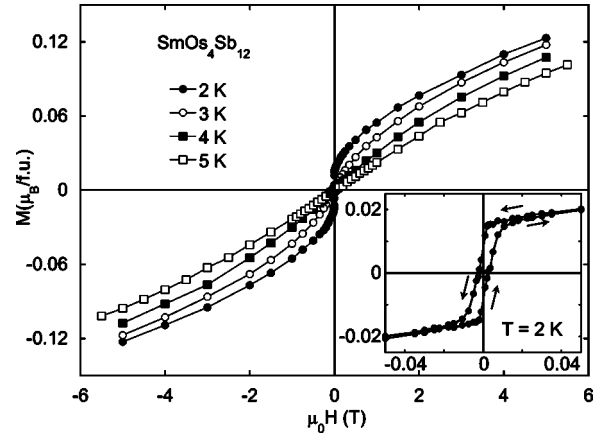

FIG. 6. $M(H)$ isotherms between -5 T and 5 T for SmOs$_4$Sb$_{12}$ at 2, 3, 4, and 5 K. The inset displays the low-field behavior of the 2 K isotherm.

was unable to describe the data. Previous work[23] has shown that $\chi(T)$ for Sm compounds can often be reasonably well described without considering CEF splitting by the equation

$$\chi(T) = \left(\frac{N_A}{k_B}\right)\left[\frac{\mu_{eff}^2}{3(T-\theta_{CW})} + \frac{\mu_B^2}{\delta}\right], \quad (2)$$

where N_A is Avogadro's number, μ_{eff} is the effective magnetic moment, θ_{CW} is the Curie-Weiss temperature, μ_B is the Bohr magneton, and $\delta=7\Delta/20$, where Δ is the energy (expressed in units of K) between the Hund's rule $J=5/2$ ground state and the $J=7/2$ first excited state. Equation (2) consists of a Curie-Weiss term due to the $J=5/2$ ground-state contribution and a temperature-independent Van Vleck term due to coupling with the first excited $J=7/2$ multiplet. The theoretical Sm^{3+} free ion moment is $\mu_{eff}=g_J[J(J+1)]^{1/2}$ $\mu_B=0.845$ μ_B/f.u., where $g_J=0.286$ is the Landé g factor and $J=5/2$. The best overall fit of Eq. (2) to the $\chi_{dc}^{-1}(T)$ data, shown in Fig. 5, results in the parameters $\theta_{CW}=-0.99$ K, $\delta=300$ K, and $\mu_{eff}=0.63$ μ_B/f.u.. The value of $\mu_{eff}=0.63$ μ_B/f.u. is somewhat less than the theoretical Sm^{3+} free ion value of $\mu_{eff}=0.845$ μ_B/f.u., while $\delta=300$ K yields $\Delta=20\delta/7=850$ K, which is much less than the $\Delta\sim1500$ K value estimated for free Sm^{3+} ions.[24] However, low values of Δ have previously been inferred from the fits to $\chi_{dc}(T)$ data for other Sm-based compounds such as SmRh$_4$B$_4$.[23]

The magnetic properties of SmOs$_4$Sb$_{12}$ were also characterized by measuring $\chi_{ac}(T)$ and $M(H,T)$ at low temperatures. The $\chi_{ac}(T)$ data (Fig. 5, inset) exhibit a peak indicative of a magnetic transition at $T_C=2.66$ K, where T_C is defined as the temperature of the midpoint of the change in χ_{ac} on the paramagnetic side. The results of isothermal $M(H)$ measurements, made in the vicinity of the transition, are shown in Fig. 6. The magnetic transition can clearly be seen in the $M(H)$ isotherms where the approximately linear behavior at 5 K becomes nonlinear at lower temperatures and hysteretic at 2 K (Fig. 6, inset). These results reveal that some type of magnetic order with a weak ferromagnetic component occurs below 2.66 K. At 2 K, the remnant magnetization M_R is $\sim0.015(1)$ μ_B/f.u. and the coercive field H_C is $\sim2.5(1)$
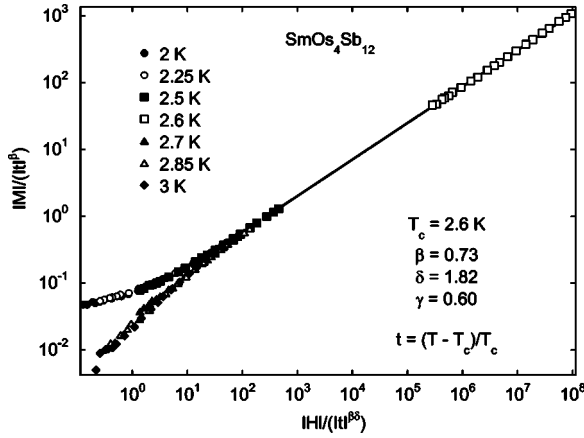
FIG. 7. Scaling plot $|M|/|t|^\beta$ vs $|H|/|t|^{\beta\delta}$ for SmOs$_4$Sb$_{12}$. The line is a guide to the eye.

FIG. 8. Modified Arrott plot for SmOs$_4$Sb$_{12}$. The inset shows the conventional Arrott plot for SmOs$_4$Sb$_{12}$ using the the critical exponents from the molecular field approximation ($\beta=1/2$ and $\gamma=1$).

$\times 10^{-3}$ T. Even though saturation is not achieved at 2 K, which is only ~0.5 K away from T_C, a magnetization value M of ~0.122(1) μ_B/f.u. is obtained at 5 T which is only 17% of the theoretical value of $M_{\text{sat}}=g_JJ$ μ_B=0.71 μ_B/f.u.

Arrott plots were constructed in an attempt to determine the Curie temperature T_C, the spontaneous magnetization M_S, and the initial susceptibility χ_0. An Arrott plot consists of M^2 vs (H/M) isotherms, where M is magnetization and H is the internal field. In general, the M^2 vs (H/M) isotherms form a series of lines for a ferromagnetic compound that are parallel near T_C, where T_C corresponds to the isotherm that passes through the origin. However, in the case of SmOs$_4$Sb$_{12}$, the M^2 vs (H/M) isotherms are strongly curved, as shown in the inset to Fig. 8. To overcome this difficulty, the $M(H,T)$ data were analyzed using a modified Arrott plot, $M^{1/\beta}$ vs $(H/M)^{1/\gamma}$ (where β and γ are critical exponents), which is based on the Arrott-Noakes equation of state.[25] To construct the modified Arrott plot, it was necessary to determine the critical exponents β and γ. This was accomplished by estimating the value of the critical exponent δ using the relation $M \sim H^{1/\delta}(T=T_C)$ and plotting $d\ln(\mu_0H)/d\ln(M)$ vs μ_0H for all the measured isotherms. The isotherm with the slope closest to zero was found to be the one for $T=2.6$ K, and the average value for $d\ln(\mu_0H)/d\ln(M)$ above μ_0H =0.05 T for this isotherm gives δ=1.82(5). These values were then analyzed using scaling theory (Fig. 7), from which $|M|/|t|^\beta$ is plotted as a function of $|H|/|t|^{\beta\delta}$ where $t=(T-T_C)/T_C$; on this plot, the isotherms collapse onto two universal curves with the isotherms for $T>T_C$ on one branch and those for $T<T_C$ on the other. Based on this scaling analysis, values of β=0.73(5) and δ=1.82(5) were determined, while γ=0.60(5) was obtained from the Widom scaling relation $\delta=1+\gamma/\beta$.[26] The resulting value of T_C from the scaling analysis is 2.60(5) K, which agrees well with T_C determined from $\chi_{\text{ac}}(T)$ measurements on the same crystal.

The critical exponents determined from the scaling analysis were then used to construct the modified Arrott plots, shown in Fig. 8. With the correct critical exponents for SmOs$_4$Sb$_{12}$, the isotherms in the modified Arrott plot were linear and parallel close to T_C in the high-field region from 0.15 to 3 T. Linear fits to the $M^{1/\beta}$ vs $(H/M)^{1/\gamma}$ data were
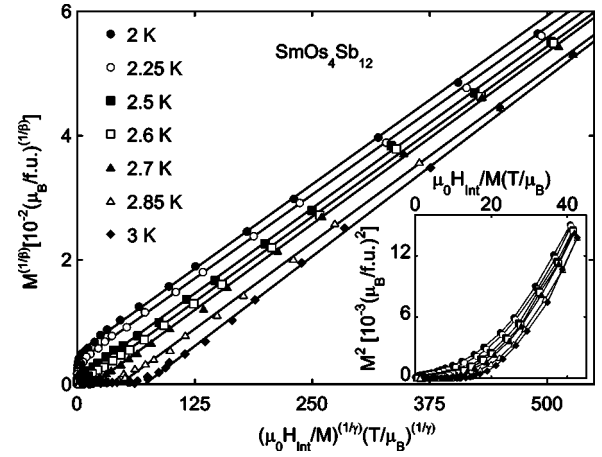
made in this field range as shown in Fig. 8; the intercepts of the fits were then used to determine the Curie temperature T_C, the initial susceptibility χ_0, and the spontaneous magnetization M_S for each isotherm. The value of T_C from the modified Arrott plots agrees well with the scaling analysis result of T_C=2.60(5) K to within ~0.1 K. A Curie-Weiss fit of $\chi_0^{-1}(T)$ [Fig. 9(a)] resulted in θ_{CW}=2.5 K and μ_{eff} =0.4 μ_B/f.u. These values are not in agreement with the earlier fit to the $\chi_{\text{dc}}^{-1}(T)$ data using Eq. (2) since the $\chi_{\text{dc}}^{-1}(T)$ data were fit from 2 to 300 K while the $\chi_0^{-1}(T)$ data were fit only near T_C.

IV. DISCUSSION

A. Crystalline electric field analysis

In the presence of a cubic crystalline electric field (CEF), the sixfold degenerate Sm^{3+} $J=5/2$ multiplet splits into a Γ_7 doublet and a Γ_8 quartet. Although it has been shown that the filling atom (Sm) in the filled skutterudites experiences tet-
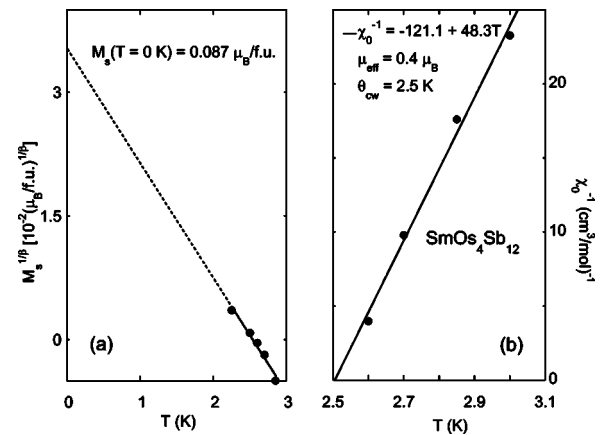

FIG. 9. (a) Spontaneous magnetization $M_S^{1/\beta}$ vs T along with a linear fit (solid line) and extrapolation to 0 K (dashed line). (b) Inverse initial susceptibility $\chi_0(T)^{-1}$ vs T along with a Curie-Weiss fit (line).
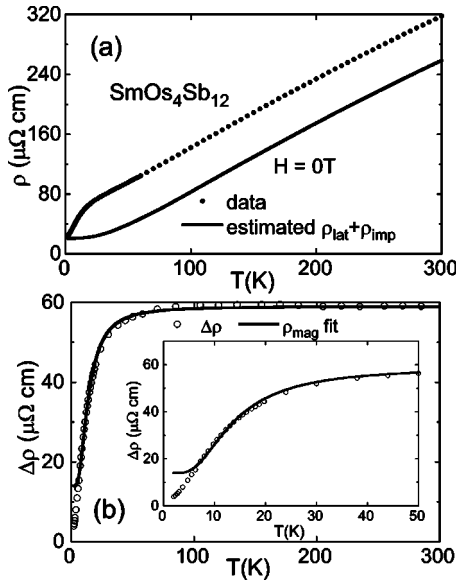
FIG. 10. (a) Zero-field electrical resistivity ρ and the estimated $\rho_{lat} + \rho_{imp}$ vs T for $SmOs_4Sb_{12}$ (sample A), where $\rho_{imp} \sim 21\ \mu\Omega$ cm. (b) $\Delta\rho (= \rho - \rho_{lat} - \rho_{imp})$ vs T compared with a fit of the resistivity due to s-f exchange scattering of electrons from the Γ_7 doublet ground state and the Γ_8 quartet excited state separated by ~ 33 K due to the CEF (solid line). The fit gives a good description of the $\Delta\rho(T)$ data from 7 to 300 K. The inset shows the quality of the fit at low temperatures.

rahedral CEF splitting,[27] cubic CEF splitting was used instead for simplicity. The best fit to the C/T data for $SmOs_4Sb_{12}$, obtained by scaling the CEF Schottky contribution by 0.58, resulted in a Γ_7 ground state and a Γ_8 excited state separated by $\Delta E \approx 38$ K. The scaling that was necessary could imply that most of the entropy of the 4f electrons in $SmOs_4Sb_{12}$ is associated with the Schottky-like anomaly while the rest resides within the heavy quasiparticles and magnetic ordering.

The zero-field electrical resistivity $\rho(T)$ of $SmOs_4Sb_{12}$ is shown in Fig. 10(a) (sample A). The resistivity $\rho(T)$ has an approximately linear-T dependence between 50 and 300 K and drops rapidly below ~ 50 K. To determine if the feature below 50 K was due to CEF splitting of the $Sm^{3+} J=5/2$ multiplet, it was necessary to subtract a lattice contribution ρ_{lat} and an impurity contribution ρ_{imp} ($\sim 21\ \mu\Omega$ cm) from the resistivity data, yielding an incremental resistivity $\Delta\rho$ (where $\Delta\rho = \rho - \rho_{lat} - \rho_{imp}$). Usually, ρ_{lat} is estimated from an isostructural nonmagnetic reference compound; in the case of $SmOs_4Sb_{12}$, $LaOs_4Sb_{12}$ was used. However, above 100 K, $\rho(T)$ of $LaOs_4Sb_{12}$ exhibits a significant amount of negative curvature, which is common in La-based compounds (such as $LaAl_2$).[28,29] The curvature is generally less pronounced in Y- and Lu-based compounds, which have empty and filled 4f-electron shells, respectively. However, since the compounds YOs_4Sb_{12} and $LuOs_4Sb_{12}$ have not yet, to our knowledge, been prepared, an estimate of ρ_{lat} for $SmOs_4Sb_{12}$ was made from 2 to 300 K. This estimate was derived by shifting the linearly T-dependent resistivity of $SmOs_4Sb_{12}$ above 100 K, where the T dependence was assumed to be completely due to electron-phonon scattering, such that it

matched smoothly with the resistivity of $LaOs_4Sb_{12}$ below 100 K. These data were then combined to represent ρ_{lat} from 2 to 300 K in Fig. 10(a). After subtracting this estimated lattice contribution, $\Delta\rho$ was plotted as shown in Fig. 10(b) and compared with the calculated resistivity due solely to s-f exchange scattering (ρ_{mag}) from the Sm^{3+} 4f energy levels in the CEF. The exchange scattering contribution ρ_{mag} for $SmOs_4Sb_{12}$ was calculated for CEF splitting of the Hund's rule $J=5/2$ multiplet for Sm^{3+}, similar to a procedure described elsewhere for $PrOs_4Sb_{12}$,[30] which was based on work by Andersen et al.[31] Since Sm^{3+} has a magnetic ground state and, in order to simplify the analysis, a contribution to the CEF resistivity due to aspherical Coulomb scattering was not considered. The fit of the calculated $\rho_{mag}(T)$ to the $\Delta\rho(T)$ data was quite good, except below ~ 7 K, where the discrepancy may be due to the ferromagnetic phase transition that occurs at ~ 2.6 K or the development of the coherent heavy Fermi liquid ground state. Based on this fit, a splitting of ~ 33 K between the Γ_7 doublet ground state and Γ_8 quartet excited state was inferred. In general, the splitting that results from the CEF fit of $\rho_{mag}(T)$ to the $\Delta\rho(T)$ data is in reasonable agreement with the value (38 K) determined from specific heat measurements. However, the possibility that the drop in the resistivity below ~ 50 K is due to the development of the coherent heavy Fermi liquid, rather than CEF splitting of the $Sm^{3+} J=5/2$ multiplet, cannot be ruled out.

The fit of Eq. (2) to the $\chi_{dc}^{-1}(T)$ data yielded a good overall description of the $\chi_{dc}(T)$ data without incorporating CEF effects. Fits that considered CEF effects in addition to the splitting between the $J=5/2$ and $J=7/2$ multiplets (not shown) did not vary significantly from the results of Eq. (2). Following the modified Arrott plot analysis, it was also found that the value of μ_{eff} determined from the fit to the $\chi_0^{-1}(T)$ data is in good agreement with $\mu_{eff} = 0.41 \mu_B$/f.u. arising from a Γ_7 ground state and is much less than $\mu_{eff} = 0.77 \mu_B$/f.u. associated with a Γ_8 ground state. However, a linear fit to $M_S^{1/\beta}(T)$ [Fig. 9(b)] resulted in a value of 0.087(1) μ_B/f.u. for M_{sat} at $T=0$ K, which is $\sim 37\%$ of $M_{sat} = g_J \langle J_z \rangle$ for a Γ_7 ground state at $T=0$ K. In addition, the failure of CEF-based fits to adequately describe the $\chi_{dc}^{-1}(T)$ data may suggest that the CEF-based fit to C/T is inappropriate. The Schottky-like anomaly at 10 K, taken to be a strong indicator of crystal field splitting, may conceivably be due to a complex temperature dependence of γ, which can occur when the value of γ is greatly enhanced,[32] as is observed in $SmOs_4Sb_{12}$.

B. Weak ferromagnetism

The low value of the magnetic entropy at the transition, the lack of features in the electrical resistivity at the transition, the low nonsaturating magnetization, and the unexplained critical exponents seem to suggest that the ferromagnetism is either unconventional, or due to an unknown impurity phase. Although an impurity phase may be responsible for the ferromagnetism, it should be noted that many compounds exhibit similar behavior, including the itinerant ferromagnets $ZrZn_2$, Ni_3Al, and Sc_3In,[33–36] many other heavy-fermion systems such as $CeNi_{0.875}Ga_{3.125}$, $YbRhSb$, and Ce_5Sn_3,[37–39] and the heavy-fermion-filled skutterudite

$SmFe_4P_{12}$.[3] For instance, the low value of the magnetic entropy at the transition ($\sim 0.016 R \ln 2$) and the small size of the feature due to magnetic ordering in C/T of $SmOs_4Sb_{12}$ are consistent with the behavior observed in weak itinerant ferromagnets such as Sc_3In.[40,41] Similar behavior is also observed in several heavy-fermion systems such as $CeNi_{0.875}Ga_{3.125}$, $YbRhSb$, Ce_5Sn_3, and $SmFe_4P_{12}$.[37–39] These heavy-fermion systems all show anomalies in C/T, although the magnetic entropy at the phase transitions of each of these systems ranges from $(0.1$ to $0.35)R \ln 2$. The lack of features in the electrical resistivity at the transition is also consistent with the weak itinerant ferromagnets $ZrZn_2$, Ni_3Al, and Sc_3In,[42–44] as well as $SmFe_4P_{12}$.[3] None of these compounds shows a clear indication of a phase transition in $\rho(T)$. In the case of the magnetization of $SmOs_4Sb_{12}$, the low nonsaturating moment is similar to behavior that has been observed in the magnetization of $SmFe_4P_{12}$, which at 1.8 K reaches a value around 0.14 μ_B/f.u. by 5 T.[3] This nonsaturating moment is also observed in weak itinerant ferromagnets, such as $ZrZn_2$, Ni_3Al, and Sc_3In.[33–36] The behavior of the systems described above is not clearly understood and has been attributed to either Kondo screening or itinerant electron magnetism.

Assuming the presence of a ferromagnetic impurity phase, the percentage of this phase present in a sample of $SmOs_4Sb_{12}$ can be estimated from the observed magnetization. Since Sm is the only magnetic constituent in $SmOs_4Sb_{12}$, it is reasonable to assume a moment of ~ 1 μ_B/f.u. for the impurity phase. In order to produce the magnetization observed at 2 K and 5 T, the impurity phase would need to constitute $\sim 1\%$ of the total mass of the crystal, assuming that the molecular weight of the impurity phase is comparable to that of Sm. Based on this, it is clear that it would be very difficult to resolve the potential impurity phase in x-ray powder diffraction data. To check whether the unconventional magnetic behavior was due to impurities in the raw materials, single crystals were grown from ultrahigh quality materials (Sm 99.99%, Os 99.999%, Sb 99.999%). Magnetization measurements made on these crystals did not differ significantly from those made on previous crystals grown from lower quality starting materials. This finding seems to indicate that if there is an impurity phase, then a Sm compound is the most likely candidate.

The applicability of the modified Arrott analysis to $SmOs_4Sb_{12}$ indicates that the ferromagnetic ordering is not described by mean-field critical exponents ($\beta = 0.5$, $\delta = 3$, and $\gamma = 1$). Deviation from mean-field behavior is not uncommon. For instance, the magnetic interactions in a given compound may be best described by other models, such as the 3D Heisenberg model for which $\beta = 0.3639$, $\delta = 4.743$, and $\gamma = 1.3873$.[45] The critical exponents determined for $SmOs_4Sb_{12}$ clearly do not agree with those of the 3D Heisenberg model, or any of the other standard models.[26] Other possible expla-

nations for the unconventional critical exponents include CEF splitting,[46] disorder of a single magnetic phase,[47,48] or the existence of multiple magnetic phases. In the case of $SmOs_4Sb_{12}$, it seems that the presence of an impurity phase could lead to the unusual critical exponents that have been observed. For example, the usual mean-field critical exponents of some ferromagnetic impurity could be obscured by the presence of a large paramagnetic contribution. However, it is also possible that the odd magnetic behavior is intrinsic to $SmOs_4Sb_{12}$ and the unexplained critical exponents may reflect some type of novel magnetic ordering. Neutron-scattering measurements could offer insight into this possibility.

V. SUMMARY

Measurements of $C(T)$, $\rho(T,H)$, $M(H,T)$, and $\chi_{ac}(T)$ have been performed on the filled skutterudite compound $SmOs_4Sb_{12}$. The $C(T)$ measurements reveal a strongly enhanced electronic specific-heat coefficient $\gamma \approx 880$ mJ/mol K^2, indicative of a large quasiparticle effective mass $m^* \approx 170 m_e$. A fit of a possible Schottky anomaly to the $C(T)$ data indicates CEF splitting of the $Sm^{3+} J = 5/2$ sixfold degenerate Hund's rule multiplet into a Γ_7 doublet ground state and a Γ_8 quartet excited state separated by 38 K. The electrical resistivity has a strong temperature dependence below ~ 50 K. CEF fits to this region agree well with the specific-heat measurements and yield an energy splitting of ~ 33 K between the Γ_7 doublet ground state and the Γ_8 quartet excited state. The resistivity of $SmOs_4Sb_{12}$ increases with field at all temperatures. Below ~ 10 K and up to 4 T, the resistivity exhibits Fermi-liquid behavior. Fits to the $\chi_{dc}^{-1}(T)$ data using a temperature-independent Van Vleck term yield a value of $\mu_{eff} = 0.634$ μ_B/f.u. with an energy gap $\Delta = 854$ K between the $J = 5/2$ and the $J = 7/2$ multiplets. The hysteresis observed in $M(H)$ at 2 K, the low value of the ordered moment, and conformity of the $M(H,T)$ data to a modified Arrott plot are consistent with weak ferromagnetic order possibly due to an impurity phase. Analysis using scaling theory and modified Arrott plots yield the values $T_C \approx 2.60(5)$ K and a spontaneous magnetization at 0 K of 0.087 μ_B/f.u.

[1] G. P. Meisner, Physica B & C **108**, 763 (1981).

[2] E. D. Bauer, N. A. Frederick, P.-C. Ho, V. S. Zapf, and M. B. Maple, Phys. Rev. B **65**, 100506(R) (2002).

[3] N. Takeda and M. Ishikawa, J. Phys.: Condens. Matter **15**, L229 (2003).

[4] E. D. Bauer, A. Ślebarski, E. J. Freeman, C. Sirvent, and M. B. Maple, J. Phys.: Condens. Matter **13**, 4495 (2001).

[5] N. R. Dilley, E. J. Freeman, E. D. Bauer, and M. B. Maple, Phys. Rev. B **58**, 6287 (1998).

[6] W. Jeitschko and D. Braun, Acta Crystallogr., Sect. B: Struct. Crystallogr. Cryst. Chem. **33**, 3401 (1977).

[7] W. Jeitschko, A. J. Foecker, D. Paschke, M. V. Dewalsky, C. B. H. Evers, B. Künnen, A. Lang, G. Kotzyba, U. C. Rodewald, and M. H. Möller, Z. Anorg. Allg. Chem. **626**, 1112 (2000).

[8] C. Sekine, T. Uchiumi, I. Shirotani, and T. Yagi, AIRAPT **17**, 826 (2000).

[9] N. Takeda and M. Ishikawa, Physica B **329–333**, 460 (2003).

[10] R. Giri, C. Sekine, Y. Shimaya, I. Shirotani, K. Matsuhira, Y. Doi, Y. Hinatsu, M. Yokoyama, and H. Amitsuka, Physica B **329–333**, 458 (2003).

[11] K. Fujiwara, K. Ishihara, K. Miyoshi, J. Takeuchi, C. Sekine, and I. Shirotani, Physica B **329–333**, 476 (2003).

[12] M. Yoshizawa, Y. Nakanishi, T. Kumagai, M. Oikawa, C. Sekine, and I. Shirotani, J. Phys. Soc. Jpn. **73**, 315 (2004).

[13] K. Matsuhira, Y. Hinatsu, C. Sekine, T. Togashi, H. Maki, I. Shirotani, H. Kitazawa, T. Takamasu, and G. Kido, J. Phys. Soc. Jpn. **71**, 237 (2002).

[14] M. E. Danebrock, C. B. H. Evers, and W. Jeitschko, J. Phys. Chem. Solids **57**, 381 (1996).

[15] M. B. Maple, N. A. Frederick, P.-C. Ho, W. M. Yuhasz, T. A. Sayles, N. P. Butch, J. R. Jeffries, and B. J. Taylor, in *Proceedings of SCES'94* [Physica B (to be published)].

[16] NONIUS KAPPA CCD package COLLECT, DENZO, SCALEPACK, SORTAV, Nonius Delft, The Netherlands, 1998.

[17] G. M. Sheldrick, SHELXS-97, Program for Crystal Structure Refinements, University of Göttingen, Germany, 1997; windows version by McArdle, Natl. Univ. Galway, Ireland.

[18] B. C. Sales, D. Mandrus, and R. K. Williams, Science **272**, 1325 (1996).

[19] E. Bauer, S. Berger, C. Paul, M. D. Mea, G. Hilscher, H. Michor, M. Reissner, W. Steiner, A. Grytsiv, P. Rogl, and E. W. Scheidt, Phys. Rev. B **66**, 214421 (2002).

[20] K. Kadowaki and S. B. Woods, Solid State Commun. **58**, 307 (1986).

[21] N. Tsujii, K. Yoshimura, and K. Kosuge, J. Phys.: Condens. Matter **15**, 1993 (2003).

[22] H. Kontani, J. Phys. Soc. Jpn. **73**, 515 (2004).

[23] H. C. Hamaker, L. D. Woolf, H. B. MacKay, Z. Fisk, and M. B. Maple, Solid State Commun. **32**, 289 (1979).

[24] J. H. Van Vleck, *The Theory of Electric and Magnetic Susceptibilities* (Oxford University Press, London, 1932).

[25] A. Arrott and J. E. Noakes, Phys. Rev. Lett. **19**, 786 (1967).

[26] J. J. Binney, N. J. Dowrick, A. J. Fisher, and M. E. J. Newman, *The Theory of Critical Phenomena* (Oxford University Press, New York, 1992).

[27] K. Takegahara, H. Harima, and A. Yanase, J. Phys. Soc. Jpn. **70**, 1190 (2001).

[28] A. Ślebarski and D. Wohlleben, Z. Phys. B: Condens. Matter **60**, 449 (1985).

[29] M. B. Maple, Ph.D. thesis, University of California, San Diego, 1969.

[30] N. A. Frederick and M. B. Maple, J. Phys.: Condens. Matter **15**, 4789 (2003).

[31] N. H. Andersen, P. E. Gregers-Hansen, E. Holm, H. Smith, and O. Vogt, Phys. Rev. Lett. **32**, 1321 (1974).

[32] G. R. Stewart, Rev. Mod. Phys. **56**, 755 (1984).

[33] S. Foner, E. J. McNiff, and V. Sadagopan, Phys. Rev. Lett. **19**, 1233 (1967).

[34] S. Ogawa, Phys. Lett. **25**, 516 (1967).

[35] F. R. de Boer, C. J. Schinkel, J. Biesterbos, and S. Proost, J. Appl. Phys. **40**, 1049 (1969).

[36] J. Grewe, J. S. Schilling, K. Ikeda, and K. A. Gschneidner, Jr., Phys. Rev. B **40**, 9017 (1989).

[37] E. V. Sampathkumaran, K. Hirota, I. Das, and M. Ishikawa, Phys. Rev. B **47**, 8349 (1993).

[38] Y. Muro, Y. Haizaki, M. S. Kim, K. Umeo, H. Tou, M. Sera, and T. Takabatake, Phys. Rev. B **69**, 020401(R) (2004).

[39] J. M. Lawrence, M. F. Hundley, J. D. Thompson, G. H. Kwei, and Z. Fisk, Phys. Rev. B **43**, 11 057 (1991).

[40] K. Ikeda and K. A. Gschneidner, Jr., J. Magn. Magn. Mater. **22**, 207 (1981).

[41] K. Ikeda and K. A. Gschneidner, Jr., J. Magn. Magn. Mater. **30**, 273 (1983).

[42] S. Ogawa, J. Phys. Soc. Jpn. **40**, 1007 (1976).

[43] C. J. Fuller, C. L. Lin, T. Mihalisin, F. Chu, and N. Bykovetz, Solid State Commun. **83**, 863 (1992).

[44] Y. Masuda, T. Hioki, and A. Oota, Physica B & C **91**, 291 (1977).

[45] K. Chen, A. M. Ferrenberg, and D. P. Landau, Phys. Rev. B **48**, 3249 (1993).

[46] K. U. Neumann and K. R. A. Ziebeck, J. Magn. Magn. Mater. **140**, 967 (1995).

[47] A. Aharoni, J. Magn. Magn. Mater. **58**, 297 (1986).

[48] I. Yeung, R. M. Roshko, and G. Williams, Phys. Rev. B **34**, 3456 (1986).